AUT Journal of Electrical Engineering

AUT J. Elec. Eng., 53(2) (2021) 159-170
DOI: 10.22060/eej.2021.19273.5388

Designing Cost- and Energy-Efficient Cell-free Massive MIMO Network with Fiber and FSO Fronthaul Links

P. Agheli, M. Javad Emadi*, H. Beyranvand

Electrical Engineering Department, Amirkabir University of Technology, Tehran, Iran

ABSTRACT: The emerging cell-free massive multiple-input multiple-output (CF-mMIMO) is a promising scheme to tackle the capacity crunch in wireless networks. Designing the optimal fronthaul network in the CF-mMIMIO is of utmost importance to deploy a cost and energy-efficient network. In this paper, we present a framework to optimally design the fronthaul network of CF-mMIMO utilizing optical fiber and free space optical (FSO) technologies. We study an uplink data transmission of the CF-mMIMO network, wherein each of the distributed access points (APs) is connected to a central processing unit (CPU) through a capacity-limited fronthaul, which could be the optical fiber or FSO. Herein, we have derived achievable rates and studied the network's energy efficiency in the presence of power consumption models at the APs and fronthaul links. Although an optical fiber link has a larger capacity, it consumes less power and has a higher deployment cost than tan FSO link. For a given total number of APs, the optimal number of optical fiber and FSO links and the optimal capacity coefficient for the optical fibers are derived to maximize the system's performance. Finally, the network's performance is investigated through numerical results to highlight the effects of different types of optical fronthaul links.

Review History:

Received: Nov. 17, 2020
Revised: Jan .31, 2021
Accepted: Feb. 03, 2021
Available Online: Sep. 01, 2021

Keywords:

Cell-free massive multiple-input multiple-output
capacity-limited optical fronthaul
achievable uplink rate
cost efficiency
and energy efficiency

1- INTRODUCTION

One of the main aspects of the emerging generations of wireless networks is to support the growing number of mobile users with high data rate demands. The massive multiple-input multiple-output (mMIMO) provides remarkable improvements in spectral and energy-efficiency. More interestingly, it accompanies near-optimal linear processing due to the weak law of large numbers [1]. Besides, thanks to the uplink and downlink channel reciprocity in the time-division duplex (TDD) transmission scheme, it is only required to know the channel state information (CSI) at the base station, and the user only needs to know the statistical average of the effective channel. Thus, the pilot transmission overhead in the downlink is relaxed. Due to the mMIMO scheme's importance, various variations of the scheme are also presented in the literature [2-4], especially, cell-free massive MIMO (CF-mMIMO) is also introduced to not only capture the gain of mMIMO scheme but also serve users with almost the same quality [3].

In the cell-free massive MIMO network, all access points (APs) concurrently serve all user equipments (UEs) in the same time-frequency resource. Thus, it provides higher data rates and wider coverage area since there are closer APs to the served UEs. For instance, the 95% likely network throughput of the cell-free massive MIMO downlink is about seven times higher than that of the small-cell without shadow fading correlation [3]. The CF-mMIMO networks are analyzed in the literature from different perspectives. The power control mechanisms for data and pilot transmissions are considered in [3] and [5]. The user-centric approach is also introduced and analyzed in [6]. The user-centric massive MIMO network offers higher per-user data rates in comparison to the CF-mMIMO approach with less backhaul overhead demand [7, 8]. Moreover, [9] and [10] have studied energy efficiency and total power consumption models at APs and backhaul links in CF-mMIMO network, where it is assumed that backhaul links are ideal. In contrast, spectral- and energy-efficiency expressions are also analyzed for limited-capacity fronthaul CF-mMIMO networks in [11, 12], and the quantization effects on the performance are studied.

In practice, the optical fiber is primarily used for fronthaul and backhaul links due to its high data capacity and low path-loss, which comes at the disadvantage of high deployment cost. Although the free space optical (FSO) technology still offers large enough data capacity with much lower deployment cost and fast setup time, it has drawbacks such as pointing error, atmospheric-dependent channel quality, and needing line-of-sight (LOS) connection [13, 14]. To address the outage problem of the FSO links in adverse atmospheric conditions, the combined radio frequency (RF) and FSO solution is employed for fronthaul and backhaul links, namely hybrid RF/FSO and relay-based cooperation [15-17]. Moreover, [18] has studied the joint deployment of RF

*Corresponding author's email: mj.emadi@aut.ac.ir

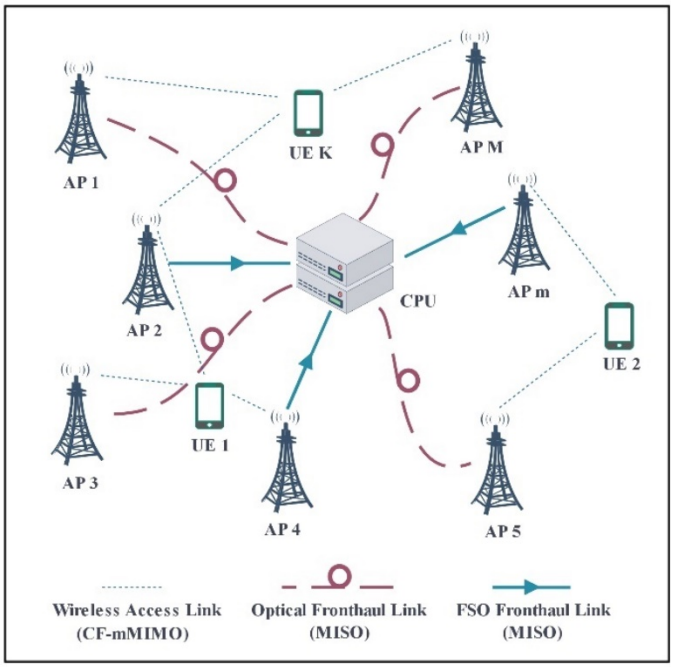

Fig. 1. CF-mMIMO wireless network with fiber and FSO fronthaul links.

and FSO fronthaul links in the uplink of a cloud-radio access network (C-RAN), and [19] presents a C-RAN network with RF multiple-access links and hybrid RF/FSO fronthaul links wherein RF-based fronthaul and multiple-access links exploit the same frequency band with the optimized time-division mechanism. Recently, CF-mMIMO network for an indoor visible light communications (VLC) is investigated in [20, 21] without considering the limited-capacity fronthaul/backhaul links effects. Recently, the uplink cell-free and user-centric mMIMO networks with radio/FSO fronthaul and multi-core fiber (MCF) backhaul links have been investigated in [22], where the optimal power allocation and adaptive fronthaul assignment have been proposed. On the other hand, meeting the increase of the wireless networks' densification and required bandwidth, the third generation partnership project (3GPP) has evolved an integrated access and backhaul (IAB) architecture at millimeter waves (mmWaves) for the fifth generation of cellular networks (5G). To this end, the same infrastructure and resources are employed for both the access and backhaul links [23, 24]. In this case, the power and spectrum allocation, distributed path selection, and bandwidth partitioning in IAB-enabled small-cell networks have been studied in [25-27].

In this paper, we analyse a cost and energy-efficient cell-free massive MIMO network with capacity-limited optical fronthaul links connecting distributed APs to the central processing unit (CPU). It is assumed that each of the fronthaul links is deployed based on optical fiber or free space optical technology according to optimal fronthaul allocation mechanism. The main contributions of the paper are summarized as follows:

· Closed-form uplink achievable data rates have been derived by employing maximum-ratio combining (MRC) and use-and-then-forget (UatF) techniques.

· To optimally design the fronthaul network, we derive closed-form spectral and energy efficiency expressions of the network by considering the fiber and the FSO deployment cost functions, power consumption models at APs, and consumed power for data transmission over the fronthaul links.

· We derive closed-form expressions for the optimal capacity coefficient of the fibers and the optimal number of fiber and FSO fronthaul links for a given number of APs by maximizing the network's energy efficiency.

· The network's performance is compared for different deployment sets of the fibers' capacity coefficient and the number of fiber-based fronthaul links from different viewpoints through extensive numerical results.

Organization: In Section 2, cell-free massive MIMO network with optical fronthaul links is introduced. Uplink achievable data rates and energy efficiency are derived in Section 3. Section 4 presents the fronthaul link allocation optimization problem, and numerical results and discussions are represented in Section 5. Finally, the paper is concluded in Section 6.

Notation: $x \in \mathbb{C}^{n\times 1}$ denotes a vector in an n-dimensional complex space, $\mathbb{E}\{.\}$ is the expectation operator, and $[.]^{\mathrm{T}}$ stands for the transpose. Additionally, $y \sim \mathcal{N}(m,\sigma^2)$ and $z \sim \mathcal{CN}(m,\sigma^2)$ denote real-valued and complex symmetric Gaussian random variables (RVs) with the m mean and the σ^2 variance.

2- SYSTEM MODEL

We assume a wireless cell-free massive MIMO (CF-mMIMO) network to simultaneously serve K UEs by M distributed APs in the same time-frequency resources. The system model is depicted in Fig. 1. All UEs and APs are

assumed to be single-antenna[1] and distributed over a large area. Each AP is connected to a CPU via a fronthaul link. Two types of fronthaul links are considered, FSO and optical fiber (OF), where M_{FSO} of the APs are connected to the CPU via the FSO links and the rest, i.e., $M_{\text{OF}} = M - M_{\text{FSO}}$, are connected via the optical fiber links. Moreover, it is assumed that the information capacity for OF (C_{OF}) is N times of that of FSO (C_{FSO}), i.e., $C_{\text{OF}} = NC_{\text{FSO}}$ for $N \geq 1$, to consider a higher capacity for the fiber links at the cost of more deployment costs than the FSO. We assume that the CPU has full-CSI, and we only focus on the uplink data transmission throughout the paper to analyse the performance of the system and the effects of fronthaul types.

2.1. Channel Model

The wireless channel between the k th UE and the m th AP follows the flat-fading model and is given by:

$$g_{mk} = \beta_{mk}^{1/2} h_{mk}, \tag{1}$$

where β_{mk} and h_{mk} represent large- and small-scale fading coefficients [3, 11, 22]. The small-scale fading coefficients h_{mk} for $m = 1,2,...,M$ and $k = 1,2,...,K$, are independent and identically distributed (i.i.d.) zero-mean complex Gaussian random variables with unit variance, i.e., $h_{mk} \sim \mathcal{CN}(0,1)$.

2.2. Uplink Data Transmission

In the uplink data transmission, all K UEs simultaneously transmit their data to APs on the same time-frequency resource element. Thus, the m th AP receives the following superimposed signal

$$y_m = \sqrt{\rho_u} \sum_{k=1}^{K} \sqrt{\eta_k} g_{mk} q_k + \omega_m \tag{2}$$

where ρ_u represents the maximum transmit power of each user, $q_k \sim \mathcal{CN}(0,1)$ is the data symbol of the k th user with power control coefficient $\eta_k \in [0,1]$, and $\omega_m \sim \mathcal{CN}(0,\delta_m^2)$ denotes additive Gaussian noise at m th AP.

2.3. Rate Distortion Theory

To perfectly represent an arbitrary continuous random variable, one needs an infinite number of bits. Thus, describing it with a finite number of bits, results in distortion. This concept is analyzed in the well-known rate distortion theory [28], which is also called the vector quantization with large enough dimension. Let us assume an i.i.d. random source $X \sim P_X(x)$ with zero-mean and bounded variance $\mathbb{E}\{|X|^2\} = \sigma^2$. Thus, the rate-distortion problem is to represent the n -length i.i.d. source $\boldsymbol{X}$ with nR bits such that average distortion becomes less than D, i.e. $\mathbb{E}\{d(\boldsymbol{X}, \hat{\boldsymbol{X}})\} \leq D$, where $\hat{\boldsymbol{X}}(i)$ for $i \in \{1,2,\ldots,2^{nR}\}$ represents the quantized versions of the random source. Therefore, the rate distortion function for the X with square-error distortion and large enough n is defined as follows [28]

$$R^*(D) = \min_{P_{\hat{X}}(\hat{x}):\mathbb{E}\left(|\hat{x}-x|^2\right)\leq D} I(\hat{X};X) \text{ [bits per symbol]}, \tag{3}$$

By using a test channel $\hat{X} = X + Z$, where $Z \sim \mathcal{CN}(0,D)$ denotes the quantization noise which is independent of X, the rate distortion function $R(D) = \log_2(1+\sigma^2/D)$ is achieved [11, 28] [2].

On the other hand, we then transmit the nR-bit quantization index over a fronthaul link with channel capacity C [bits per channel use] without error. Thus, to minimize the quantization noise variance of D, we must use the maximum capacity of the fronthaul channel. Therefore, $R(D) = \log_2(1+\sigma^2/D^*) = C$, and $D^* = \frac{\sigma^2}{2^C - 1}$.

3- PERFORMANCE ANALYSIS

In the following section, we present the uplink achievable data rates. Thus, after receiving the uplink data signals at APs, each access point quantizes and forwards the signal to the CPU over its allocated fronthaul link. Then, users' data recovery is performed at the CPU, and the achievable rates are derived.

3.1. Quantization

After receiving the superimposed signal y_m given in Eq. (2) at m th AP, by use of the rate distortion theory, the AP compresses the received signal to $\hat{y}_m$. Thus, we have:

$$\hat{y}_m = y_m + n_m = \sqrt{\rho_u} \sum_{k=1}^{K} \sqrt{\eta_k} g_{mk} q_k + \omega_m + n_m \tag{4}$$

where $n_m \sim \mathcal{CN}(0, D_m)$ represents the quantization noise at m th AP which is independent of y_m. To perfectly send the quantization index over the OF fronthaul link or FSO one with capacity C_m, we have: $D_m = \frac{\mathbb{E}\{|y_m|^2\}}{2^{C_m} - 1}$. Thus, the CPU receives $\hat{y}_m$ perfectly from the m th AP.

3.2. User Data Detection

The CPU receives the compressed signals given in Eq. (4) from all the APs, and applies the MRC technique to recover the data symbols of all the users. To recover the information symbol of k th UE, i.e., q_k, we have:

1 It can be extended to a system with multi-antenna APs under more complex mathematical computations.

2 There is another variation of the test channel $X = \hat{X} + Z$ in which $Z \sim \mathcal{CN}(0,D)$ represents the quantization noise which is independent of $\hat{X}$. In this case, the rate distortion function is obtained as $R(D) = \log_2(\sigma^2/D)$ which is smaller than $R(D) = \log_2(1+\sigma^2/D)$. In the paper, based on the mathematical simplicity, we have used one of the two mentioned test channels.

$$r_k = \sum_{m=1}^{M} \hat{y}_m g_{mk}^* = \sum_{m=1}^{M} \left(\sqrt{\rho_u} \sum_{k'=1}^{K} \sqrt{\eta_{k'}} g_{mk'} q_{k'} + \omega_m + n_m \right) g_{mk}^*$$
$$= \sqrt{\rho_u} \sum_{m=1}^{M} \sum_{k'=1}^{K} \sqrt{\eta_{k'}} g_{mk'} g_{mk}^* q_{k'} + \sum_{m=1}^{M} \left(\omega_m + n_m \right) g_{mk}^* \quad (5)$$
$$= \sqrt{\rho_u} \sum_{m=1}^{M} \sqrt{\eta_k} \left| g_{mk} \right|^2 q_k$$
$$+ \sqrt{\rho_u} \sum_{m=1}^{M} \sum_{\substack{k'=1 \\ k' \neq k}}^{K} \sqrt{\eta_{k'}} g_{mk'} g_{mk}^* q_{k'} + \sum_{m=1}^{M} \left(\omega_m + n_m \right) g_{mk}^*,$$

which consists of the desired signal, multi-user interference, and noise.

3.3. User Data Detection

By applying the well-known use-and-then-forget (UatF) technique [11, 29], we can relax the availability of the full instantaneous CSI at the users. Instead, it is sufficient to know only the statistical average of the effective channel. Thus, Eq. (5) is rewritten as [22]:

$$r_k = \mathrm{DS}_k \cdot q_k + \mathrm{BU}_k \cdot q_k + \sum_{\substack{k'=1 \\ k' \neq k}}^{K} \mathrm{I}_{kk'} \cdot q_{k'} + v_k \quad (6)$$

Where:

.

DS_k is the desired signal of the k th UE:

$$\mathrm{DS}_k = \sqrt{\rho_u} \mathbb{E} \left\{ \sum_{m=1}^{M} \sqrt{\eta_k} \left| g_{mk} \right|^2 \right\} \quad (7)$$

$\cdot \mathrm{BU}_k$ denotes the beamforming uncertainty of the k th user due to the statistical knowledge of CSI:

$$\mathrm{BU}_k = \sqrt{\rho_u} \left(\sum_{m=1}^{M} \sqrt{\eta_k} \left| g_{mk} \right|^2 - \mathbb{E} \left\{ \sum_{m=1}^{M} \sqrt{\eta_k} \left| g_{mk} \right|^2 \right\} \right) \quad (8)$$

$\cdot \mathrm{I}_{kk'}$ represents the inter-user interference from k' th users:

$$\mathrm{I}_{kk'} = \sqrt{\rho_u} \sum_{m=1}^{M} \sqrt{\eta_{k'}} g_{mk'} g_{mk}^* \quad (9)$$

$\cdot v_k$ is the composition of both the additive Gaussian and the quantization noises:

$$v_k = \sum_{m=1}^{M} \left(\omega_m + n_m \right) g_{mk}^* \quad (10)$$

It can be shown that all terms given in Eq. (6) are mutually uncorrelated. From the information's theoretic point of view, to analyze the worst-case scenario we assume that all the terms, except the desired term, are modeled by an equivalent Gaussian random variable with the same variance. Thus, the uplink achievable rate [bps/Hz] of the k th user is presented as:

$$R_{u,k} = \log_2 (1 + \gamma_k) \quad (11)$$

where γ_k represents the SINR of the k th user, which is given by:

$$\gamma_k = \frac{\left| \mathrm{DS}_k \right|^2}{\mathbb{E} \left\{ \left| \mathrm{BU}_k \right|^2 \right\} + \sum_{\substack{k'=1 \\ k' \neq k}}^{K} \mathbb{E} \left\{ \left| \mathrm{I}_{kk'} \right|^2 \right\} + \mathbb{E} \left\{ \left| v_k \right|^2 \right\}} \quad (12)$$

In the following Theorem, the SINR of the k th user is computed.

Theorem 1. The k th user has the following SINR:

$$\gamma_k = \frac{\rho_u \eta_k \left(\sum_{m=1}^{M} \beta_{mk} \right)^2}{\sum_{m=1}^{M} \left(\rho_u \sum_{k'=1}^{K} \eta_{k'} \beta_{mk'} + \delta_m^2 + D_m \right) \beta_{mk}} \quad (13)$$

Proof: The proof is given in Appendix A.

4- FRONTHAUL LINK DESIGN

As mentioned in the system model, it is assumed that each AP is connected to the CPU via a fronthaul link, which could be a fiber link or a free space optical link. Although the fiber optic link has a higher channel capacity and smaller path loss compared to FSO, the deployment cost to develop the fiber link is much higher than FSO. The deployment cost refers to a sum of costs for optical transceivers, digging, installation, and medium maintenance under fiber technology, which is costlier in urban areas. In contrast, there is no need for digging and medium maintenance in the case of FSO technology, even though it demands more repeaters in urban areas. Thus, there is a trade-off between supporting higher data rates and lower deployment costs, which depends on the network's key values. Network providers should choose whether to design a system with the highest achievable data transmission rate, or a system with a lower data rate but with a lower cost. On the other hand, it is worth mentioning that due to the quantization noise added at the AP for compression, it is not clear how large must be the capacity of the fronthaul link. Therefore, in the following, we present a metric not only to consider the capacity of the fronthaul links, but also take into account the deployment cost as well to find out how many fiber and/or FSO fronthaul links must be used to maximize the energy efficiency of the system.

In the following, the energy efficiency of the system is presented. The relevant optimization problem is also discussed, which includes the total power consumption of the network and fronthaul network's deployment costs.

4.1. Energy Efficiency

The energy efficiency of the network is defined as

$$\mathrm{EE}=\frac{B_s\sum_{k=1}^{K}R_{u,k}}{P_{\text{net}}+\grave{\mathrm{U}}_{\text{fh}}}\ \text{[bit/Joule]} \tag{14}$$

where B_s is the system bandwidth and to model the fronthaul network's deployment costs, $\grave{\mathrm{U}}_{\text{fh}}=\sum_{m=1}^{M}C_m\mu_m$ is used in which μ_m [Watt/bps/Hz] represents the cost coefficient of data transmission over the fronthaul link of the m th AP which depends on the type of fronthaul link. Additionally, P_{net} represents the total power consumption of the network [9, 11], which is given by [22]:

$$P_{\text{net}}=\sum_{k=1}^{K}P_k+\sum_{m=1}^{M}P_m+B_s\sum_{m=1}^{M}C_mP_{\text{fh},m}+\sum_{m=1}^{M}P_{0,m} \tag{15}$$

where C_m denotes the fronthaul link capacity of the m th AP, and:

- $P_k=\rho_u\eta_k$ represents the uplink transmit power of the k th UE,
- P_m denotes the total consumption power of circuit elements at the m th AP,
- $P_{\text{fh},m}$ [Watt/Gbps] represents the traffic-dependent data transmission power for the fronthaul link connecting the m th AP to the CPU,
- $P_{0,m}$ is the constant traffic-independent power consumed by the fronthaul link of m th AP.

It is assumed that a fiber-based fronthaul link has a higher deployment cost and consumes less traffic-dependent data transmission power than the FSO one, i.e., $\mu_{m_{\text{FSO}}}\le\mu_{m_{\text{OF}}}$ and $P_{\text{fh},m_{\text{FSO}}}\ge P_{\text{fh},m_{\text{OF}}}$ for $m_{\text{FSO}}=1,2,...,M_{\text{FSO}}$ and $m_{\text{OF}}=M_{\text{FSO}}+1,M_{\text{FSO}}+2,...,M$.

4.2. Optimization Problem

Now, we focus on maximizing the network's energy efficiency subject to have a total number of M APs to find out how many of the fronthaul links must be fiber or FSO, and how much larger must be the capacity of the fiber link. Thus, the optimization problem is given by:

$$\mathcal{P}_1:\begin{cases}\max\limits_{M_{\text{FSO}}\ge0,M_{\text{OF}}\ge0,N\ge0}\ \mathrm{EE}\\ \text{s.t.:}\quad M_{\text{FSO}}+M_{\text{OF}}\le M.\end{cases} \tag{16}$$

By replacing M_{FSO} with $M-M_{\text{OF}}$, and plugging $R_{u,k}$ and P_{net}, i.e., Eq. (11) - Eq. (13) and Eq. (15), in $\mathcal{P}_1$, we have

$$\mathcal{P}_2:\max_{0\le M_{\text{OF}}\le M,0\le N}=\frac{B_s\sum_{k=1}^{K}\log_2\left(1+\frac{\rho_u\eta_k\left(\sum_{m=1}^{M}\beta_{mk}\right)^2}{\sum_{m=1}^{M}\left(\rho_u\sum_{k'=1}^{K}\eta_{k'}\beta_{mk'}\right)\beta_{mk}+\delta_m^2+D_m}\right)}{\sum_{k=1}^{K}\rho_u\eta_k+\sum_{m=1}^{M}P_m+B_s\sum_{m=1}^{M}C_mP_{\text{fh},m}+\sum_{m=1}^{M}P_{0,m}+\sum_{m=1}^{M}C_m\mu_m} \tag{17}$$

Without loss of generality and for the sake of simplicity, we assume that all the access links experience the same large-scale fading, i.e., $\beta_{mk}=\beta$. To simplify the optimization problem, it is assumed that the users have equal transmit powers, i.e., $\eta_k=\eta$, the FSO-based access points have the same power and cost parameters that are $\mu_{m_{\text{FSO}}}=\mu_{\text{FSO}}$ and $P_{\text{fh},m_{\text{FSO}}}=P_{\text{fh,FSO}}$ are the same for the fiber-based APs, we have $\mu_{m_{\text{OF}}}=\mu_{\text{OF}}$ and $P_{\text{fh},m_{\text{OF}}}=P_{\text{fh,OF}}$. Moreover, the variance of the additive Gaussian noise at all the access points are the same, i.e., $\delta_m^2=\delta^2$. Therefore, the optimization problem is simplified as:

$$\mathcal{P}_3:\max_{0\le M_{\text{OF}}\le M,N\ge0}=\frac{KB_s\log_2\left(1+\frac{L_1}{L_2+(M-M_{\text{OF}})\alpha_{\text{FSO}}+M_{\text{OF}}\frac{\alpha_{\text{OF}}}{2^{NC_{\text{FSO}}}-1}}\right)}{\Gamma_{ep}+(M-M_{\text{OF}})\Gamma_{\text{FSO}}+NM_{\text{OF}}\Gamma_{\text{OF}}}, \tag{18}$$

where the parameters are presented in Table 1.

In the following propositions, optimal solutions of the optimization problem $\mathcal{P}_3$ are presented.

Proposition 1. For a fixed M_{OF}, the optimal capacity coefficient of the fiber compared to that of the FSO is:

$$N^*\simeq\frac{-1}{C_{\text{FSO}}}\log_2\left(-\Gamma_{\text{OF}}\alpha_{\text{OF}}M_{\text{OF}}\lambda_1+\frac{\sqrt{\lambda_1^2-4(1-\lambda_3)\log_2\left(\frac{\lambda_2}{L_1}\right)}}{2.885\left(1-\frac{1}{\lambda_3}\right)}\right), \tag{19}$$

Where:

$$\lambda_1=2.443+\log_2\left(\frac{\lambda_2}{L_1}\right)+\frac{\lambda_4C_{\text{FSO}}}{\Gamma_{\text{OF}}M_{\text{OF}}}$$
$$\lambda_2=L_2+(M-M_{\text{OF}})\alpha_{\text{FSO}}$$
$$\lambda_3=\frac{\lambda_2}{\alpha_{\text{OF}}M_{\text{OF}}\ln(2)}$$
$$\lambda_4=\Gamma_{ep}+(M-M_{\text{OF}})\Gamma_{\text{FSO}}.$$

Proof: The proof is given in Appendix B.

Proposition 2. For a fixed N, the optimal number of fiber-based access points is

Table 1. Optimization parameters.

Parameter	Formula
L_1	$M^2\rho_u\eta\beta^2$
L_2	$MK\rho_u\eta\beta^2+M\delta^2\beta$
α_{FSO}	$\frac{\left(K\rho_u\eta\beta+\delta^2\right)}{2^{C_{\text{FSO}}}-1}\beta$
α_{OF}	$\left(K\rho_u\eta\beta+\delta^2\right)\beta$
Γ_{ep}	$K\rho_u\eta+\sum_{m=1}^{M}\left(P_m+P_{0,m}\right)$
Γ_{FSO}	$C_{\text{FSO}}\left(B_sP_{\text{fh,FSO}}+\mu_{\text{FSO}}\right)$
Γ_{OF}	$C_{\text{FSO}}\left(B_sP_{\text{fh,OF}}+\mu_{\text{OF}}\right)$

$$M_{\text{OF}}^{*}\simeq\max\left\{0,\frac{\kappa_1\kappa_4-\kappa_2\kappa_3}{2\kappa_2\kappa_4}\right\} \tag{20}$$

where

$$\kappa_1=L_2+M\alpha_{\text{OF}},\quad \kappa_2=\alpha_{\text{FSO}}-\frac{\alpha_{\text{OF}}}{2^{NC_{\text{FSO}}}-1},$$
$$\tilde{\kappa}_3=\tilde{\Gamma}_{ep}+M\tilde{\Gamma}_{\text{FSO}},\ \text{and}\ \kappa_4=N\tilde{\Gamma}_{\text{OF}}-\tilde{\Gamma}_{\text{FSO}}.$$

Proof: The proof is given in Appendix C.

As given in Eq. (20), the optimal M_{OF}^{*} is proportional to the number of total access points \$M\$. Hence, by increasing the number of APs, M_{OF}^{*} increases because κ_1 becomes larger and faster than κ_3. Furthermore, by increasing the power and cost parameters of OF-based APs, M_{OF}^{*} decreases. In contrast, by increasing the power and cost parameters of FSO-based APs, M_{OF}^{*} increases. Increasing the circuit power and fronthaul constant power consumption of the APs makes M_{OF}^{*} smaller.

5- NUMERICAL RESULTS AND DISCUSSION

In this section, we present numerical results to highlight the performance of the proposed network architecture and analyze the effects of the fronthaul links on the energy and spectral efficiency of the system. Conventionally, it is assumed that $M=100$ APs and $K=10$ UEs are uniformly and randomly distributed within the area of $D=1\times1[\text{km}]^2$. Large-scale fading is modeled by a combination of both path-loss and shadowing. Thus, it is presented by [3]:

$$\beta_{mk}=10^{\frac{\text{PL}_{\text{mk}}}{10}}10^{\frac{\sigma_{\text{sh}}z_{\text{mk}}}{10}} \tag{21}$$

where $\text{PL}_{mk}[\text{dB}]$ represents the path-loss and $10^{\frac{\sigma_{\text{sh}}z_{\text{mk}}}{10}}$ denotes the shadowing with standard deviation σ_{sh}, while z_{mk} is the shadowing correlation factor.

Path-loss model: We employ the conventional three-slope propagation model for path-loss, which is defined as [3, 11]:

$$\text{PL}_{mk}=\begin{cases}-L-35\log_{10}\left(d_{mk}\right), & d_{mk}>d_1\\ -L-15\log_{10}\left(d_1\right)-20\log_{10}\left(d_{mk}\right), & d_0<d_{mk}\le d_1\\ -L-15\log_{10}\left(d_1\right)-20\log_{10}\left(d_0\right), & d_{mk}\le d_0\end{cases} \tag{22}$$

where d_0 and d_1 are two distance measuring references, d_{mk} represents the distance between m th AP and k th UE, and:

$$L=46.3+33.9\log_{10}(f)-13.82\log_{10}\left(h_{\text{AP}}\right)$$
$$-\left(1.1\log_{10}(f)-0.7\right)h_{\text{UE}}+\left(1.56\log_{10}(f)-0.8\right)[\text{dB}], \tag{23}$$

where $f[\text{MHz}]$ denotes access radio frequency, $h_{\text{AP}}[\text{m}]$ and $h_{\text{UE}}[\text{m}]$ are the heights of the AP and UE.

Shadowing model: Due to the short distance between APs and UEs in the cell-free network, the same obstacles may exist around the APs and the UEs, which affects the shadowing characteristics. Therefore, the correlated shadowing model is suggested in [3], and the shadowing correlation represented by two parameters:

$$z_{mk}=\sqrt{\vartheta}a_m+\sqrt{1-\vartheta}b_k \tag{24}$$

Table 2. Network parameters for numerical results.

Parameter	Symbol	Value
Access radio frequency	f	1.9[GHz]
System bandwidth	B_s	20[MHz]
Antenna height of AP	h_{AP}	15[m]
Antenna height of UE	h_{UE}	1.65[m]
Path-loss model minimum distance	d_0	10[m]
Path-loss model maximum distance	d_1	50[m]
Shadowing standard deviation	σ_{sh}	8[dB]
Shadowing correlation coefficient	ϑ	0.5
UE's maximum transmission power	ρ_u	100[mWatt]
UE's power control coefficient	η	0.5
Capacity of FSO-based fronthaul	C_{FSO}	2[bps/Hz]
Circuit power at m th AP	P_m	0.2[Watt]
Fronthaul's constant power at m th AP	$P_{0,m}$	0.825[Watt]
FSO-based fronthaul's traffic-dependent power	$P_{\text{fh,FSO}}$	0.3[Watt/Gbps]
OF-based fronthaul's traffic-dependent power	$P_{\text{fh,OF}}$	0.25[Watt/Gbps]
FSO-based fronthaul's cost coefficient	μ_{FSO}	0.003[Watt/bps/Hz]
OF-based fronthaul's cost coefficient	μ_{OF}	0.03[Watt/bps/Hz]
Noise power at each AP	δ^2	$k_B T_0 B_s NF$
Boltzmann constant	k_B	1.381×10^{-23}[dB]
Noise temperature	T_0	290[Kelvin]
Noise figure	NF	9[dB]

where $\vartheta \in [0,1]$, $a_m \sim \mathcal{N}(0,1)$ and $b_k \sim \mathcal{N}(0,1)$ are independent random variables which model contribution to the shadowing due to the obstacles near to APs and the ones close to the UEs. If one sets $\vartheta = 0$, the shadowing caused by each UE becomes equal at all APs, and for $\vartheta = 1$, the shadowing caused by each AP becomes similar for all UEs. The parameters used for the numerical results are presented in Table 2; otherwise, they are clearly mentioned in the paper.

The network energy efficiency versus M_{OF} and N is depicted in Fig. 2. It is shown that increasing N at large values of M_{OF} improves energy efficiency and then continuously decreases. For instance, at $\mu_{\text{OF}} = 0.03$[Watt/bps/Hz] and $\mu_{\text{FSO}} = 0.003$[Watt/bps/Hz], the energy efficiency has a global optimum at $M^*_{\text{OF}} = 48$ and $N^* = 2$. Additionally, the same behavior is observed with slower changes for the small values of M_{OF}. To study the effect of deployment cost on the network's energy efficiency, we have compared different sets of cost parameters for OF- and FSO-based fronthaul links. If it is possible to reduce the cost of fiber links, it would be better to use more fibers than the FSO links. Thus, optimizing the network performance highly depends on efficiently selecting the fronthaul links.

The energy efficiency versus M_{OF} is represented for different values of N, i.e., different fiber capacity, in Fig. 3. By increasing the value of N, the optimal point of M_{OF} decreases; For instance, at $N \geq 8$, using FSO technology for all the fronthaul links is optimal, (i.e. $M^*_{\text{OF}} = 0$). Moreover, when the capacity limit of both FSO and OF links are the same (i.e. $N = 1$), the same scenario occurs because the deployment cost of an FSO link is much smaller than an OF link. On the other hand, to maximize the energy efficiency, it is optimal to use $N = 2$ and $M_{\text{OF}} = 48$.

The cumulative distribution functions of uplink sum-rate and uplink per-user rate are presented in Fig. 4(a) and Fig. 4(b). Here, we have compared the network performance for different capacity coefficients and the relevant optimal number of OF-based access points. It is shown that the network implemented based on the globally optimum values of N

and M_{OF} provides the highest uplink rates in comparison to the other sub-optimal setups.

Fig. 5 presents the energy efficiency versus the uplink sum-rate for different values of the capacity coefficient. At a particular amount of uplink sum-rate (e.g. $22[\mathrm{bps/Hz}]$), since the total power consumption of the network, given in Eq. (15) is proportional to the value of capacity coefficient, the performance degrades by increasing N. Moreover, to maximize the performance of the system it is not efficient to use very high-capacity fibers.

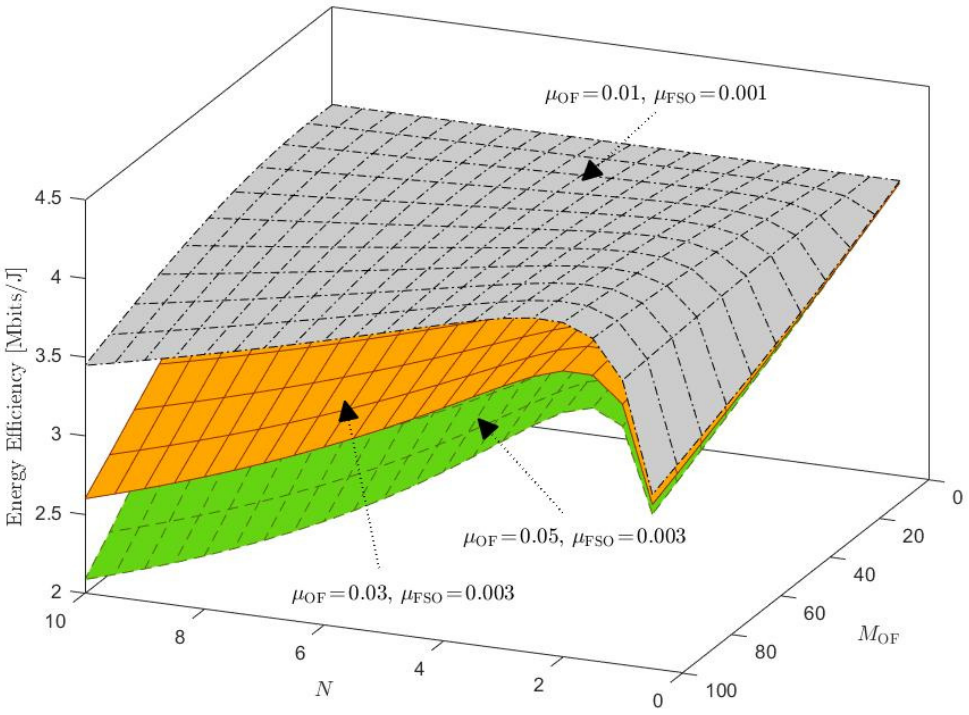

Fig. 2. Impact of the different values of cost parameters on energy efficiency of the network.

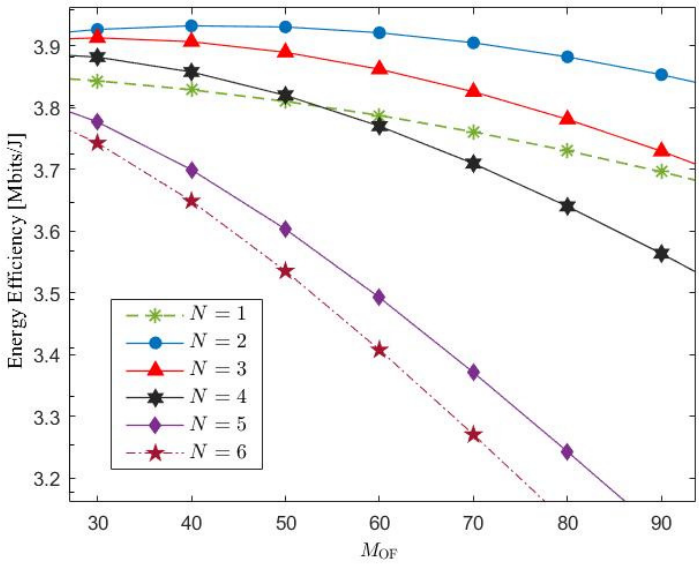

Fig. 3. Energy efficiency of the system versus M_{OF}.

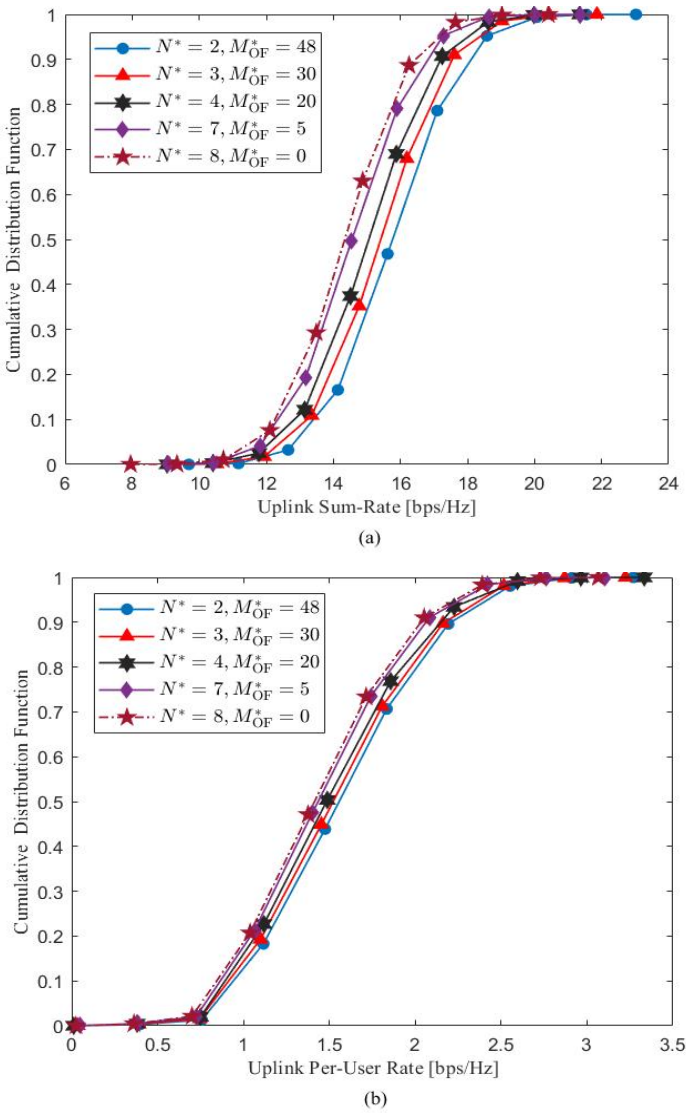

Fig. 4. CDF of (a) uplink sum-rate and (b) uplink per-user rate.

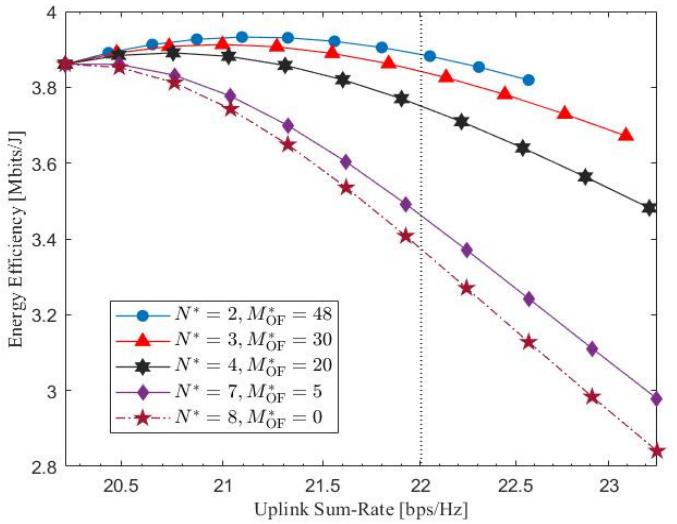

Fig. 5. Energy efficiency versus uplink sum-rate.

6- CONCLUSION

We studied the uplink of the cell-free massive MIMO network with capacity-limited fiber and FSO fronthaul links. First we represented the system and channel models. Next, data recovery and uplink data rates were analyzed. Eventually, an optimal fronthaul link design was proposed to maximize the network's energy efficiency subject to the total number of the APs. With the fronthaul link design, we obtained the optimal number of APs with fiber fronthauling and each fiber link's desired capacity compared to an FSO link for a cost and energy-efficient network. Subsequently, the number of APs with FSO fronthaul links were acquired. The network's energy and spectral efficiency were discussed through numerical results to clarify the need for optimal fronthaul allocations. The results show that the network's energy efficiency reaches its highest value by considering $N^* = 2$ and $M_{\text{OF}}^* = 48$ the optimal values. Even though higher fiber capacities provide faster data transfer, it increases the deployment cost. Thus, we have $M_{\text{OF}} \le M_{\text{OF}}^*$, for $N \ge N^*$, to ensure high energy and spectral efficiency with reasonable deployment cost.

Appendix A.

To derive the SINR, in the following after a sequence of mathematical manipulations, we derive the variances of each term given in Eq. (12).

· Computation of DS_k: Since the channel coefficients are i.i.d., we obtain:

$$\text{DS}_k = \sqrt{\rho_u \eta_k} \sum_{m=1}^{M} \mathbb{E}\left\{ \left| g_{mk} \right|^2 \right\} = \sqrt{\rho_u \eta_k} \sum_{m=1}^{M} \beta_{mk} \tag{25}$$

· Computation of $\mathbb{E}\{|\,\text{BU}_k\,|^2\}$: As the variance of a sum of independent random variables is equal to the sum of the variances, we have:

$$\begin{aligned} \mathbb{E}\left\{ \left| \text{BU}_k \right|^2 \right\} &= \rho_u \eta_k \sum_{m=1}^{M} \mathbb{E}\left\{ \left| \| g_{mk} \right|^2 - \mathbb{E}\left\{ \left| g_{mk} \right|^2 \right\} \right|^2 \right\} \\ &= \rho_u \eta_k \sum_{m=1}^{M} \left\{ \mathbb{E}\left\{ \left| \| g_{mk} \right|^2 \right|^2 \right\} - \left| \mathbb{E}\left\{ \left| g_{mk} \right|^2 \right\} \right|^2 \right\} \\ &= \rho_u \eta_k \sum_{m=1}^{M} \left\{ \mathbb{E}\left\{ \left| g_{mk} \right|^4 \right\} - \beta_{mk}^2 \right\} \\ &= \rho_u \eta_k \sum_{m=1}^{M} \left\{ 2\beta_{mk}^2 - \beta_{mk}^2 \right\} \\ &= \rho_u \eta_k \sum_{m=1}^{M} \beta_{mk}^2 . \end{aligned} \tag{26}$$

· Computation of $\mathbb{E}\{|\,\text{I}_{kk'}\,|^2\}$: Since the channel coefficients are i.i.d., we have:

$$\mathbb{E}\left\{ \left| \text{I}_{kk'} \right|^2 \right\} = \rho_u \eta_{k'} \sum_{m=1}^{M} \mathbb{E}\left\{ \left| g_{mk'} g_{mk}^* \right|^2 \right\} = \rho_u \eta_{k'} \sum_{m=1}^{M} \beta_{mk'} \beta_{mk} \tag{27}$$

.

Computation of $\mathbb{E}\{|\,v_k\,|^2\}$: It can be shown that the additive Gaussian noise and the quantization noise are mutually uncorrelated, and both are uncorrelated with the channel coefficients. Thus:

$$\mathbb{E}\left\{ \left| v_k \right|^2 \right\} = \sum_{m=1}^{M} \mathbb{E}\left\{ \left| \left(\omega_m + n_m \right) g_{mk}^* \right|^2 \right\} = \sum_{m=1}^{M} \left(\delta_m^2 + D_m \right) \beta_{mk} \tag{28}$$

By plugging Eq. (25), Eq. (26), Eq. (27), and Eq. (28) into Eq. (12), we obtain the SINR as given in Eq. (13).

Appendix B.

To compute the optimal value of the capacity coefficient, we investigate the optimization problem $\mathcal{P}_3$. Without loss of generality, the constant parameter KB_s is ignored. Hence we have:

$$\mathcal{P}_4 : \max_{0 \le M_{\text{OF}} \le M, N \ge 0} \Lambda\left(N, M_{\text{OF}} \right), \tag{29}$$

Where:

$$\Lambda\left(N, M_{\text{OF}} \right) = \frac{\log_2 \left(1 + \dfrac{L_1}{L_2 + \left(M - M_{\text{OF}} \right) \alpha_{\text{FSO}} + M_{\text{OF}} \dfrac{\alpha_{\text{OF}}}{2^{NC_{\text{FSO}}} - 1}} \right)}{\Gamma_{ep} + \left(M - M_{\text{OF}} \right) \Gamma_{\text{FSO}} + N M_{\text{OF}} \Gamma_{\text{OF}}}, \tag{30}$$

Since the fiber channel capacity is large enough, we have $2^{NC_{\text{FSO}}} \gg 1$ for the large values of NC_{FSO}. Hence, Eq. (30) reduces to:

$$\begin{aligned} \Lambda\left(N, M_{\text{OF}} \right) &= \frac{\log_2 \left(\dfrac{L_1}{L_2 + \left(M - M_{\text{OF}} \right) \alpha_{\text{FSO}} + M_{\text{OF}} \alpha_{\text{OF}} 2^{-NC_{\text{FSO}}}} \right)}{\Gamma_{ep} + \left(M - M_{\text{OF}} \right) \Gamma_{\text{FSO}} + N M_{\text{OF}} \Gamma_{\text{OF}}} \\ &= \frac{-\log_2 \left(\dfrac{L_2 + \left(M - M_{\text{OF}} \right) \alpha_{\text{FSO}} + M_{\text{OF}} \alpha_{\text{OF}} 2^{-NC_{\text{FSO}}}}{L_1} \right)}{\Gamma_{ep} + \left(M - M_{\text{OF}} \right) \Gamma_{\text{FSO}} + N M_{\text{OF}} \Gamma_{\text{OF}}}. \end{aligned} \tag{31}$$

To find the optimal value of N for a given M_{OF}, we compute the following first derivative:

$$\begin{aligned}\frac{d}{dN}\left\{\Lambda\left(N,M_{\mathrm{OF}}\right)\right\}&\overset{(a)}{=}-\frac{d}{dN}\left\{\frac{\log_2\left(\dfrac{\lambda_2+M_{\mathrm{OF}}\alpha_{\mathrm{OF}}2^{-NC_{\mathrm{FSO}}}}{L_1}\right)}{\lambda_4+NM_{\mathrm{OF}}\Gamma_{\mathrm{OF}}}\right\}\\&\overset{(b)}{=}\left(\lambda_4+NM_{\mathrm{OF}}\Gamma_{\mathrm{OF}}\right)\frac{\alpha_{\mathrm{OF}}C_{\mathrm{FSO}}2^{-NC_{\mathrm{FSO}}}}{\lambda_2+M_{\mathrm{OF}}\alpha_{\mathrm{OF}}2^{-NC_{\mathrm{FSO}}}}\\&+\Gamma_{\mathrm{OF}}\log_2\left(\frac{\lambda_2}{L_1}\right)+\Gamma_{\mathrm{OF}}\log_2\left(1+\frac{\alpha_{\mathrm{OF}}M_{\mathrm{OF}}}{\lambda_2}2^{-NC_{\mathrm{FSO}}}\right)\\&\overset{(c)}{\approx}\left(\lambda_4+NM_{\mathrm{OF}}\Gamma_{\mathrm{OF}}\right)\frac{\alpha_{\mathrm{OF}}C_{\mathrm{FSO}}2^{-NC_{\mathrm{FSO}}}}{\lambda_2+M_{\mathrm{OF}}\alpha_{\mathrm{OF}}2^{-NC_{\mathrm{FSO}}}}\\&+\Gamma_{\mathrm{OF}}\log_2\left(\frac{\lambda_2}{L_1}\right)+\Gamma_{\mathrm{OF}}\frac{\alpha_{\mathrm{OF}}M_{\mathrm{OF}}}{\lambda_2}2^{-NC_{\mathrm{FSO}}},\end{aligned}\tag{32}$$

where (a) is due to replacing of the defined parameters given in Eq. (19) into Eq. (31), and (b) is valid for differentiating and some simplifications. By using $\ln(1+x)\approx x$ for $x\ll 1$, (c) holds due to $2^{NC_{\mathrm{FSO}}}\gg 1$.

Now, by defining $\chi := 2^{-NC_{\mathrm{FSO}}}$ and using Eq. (), we have:

$$\left(\lambda_4+\frac{\Gamma_{\mathrm{OF}}M_{\mathrm{OF}}}{C_{\mathrm{FSO}}\ln(2)}(1-\chi)\right)\frac{\alpha_{\mathrm{OF}}C_{\mathrm{FSO}}\chi}{\lambda_2+M_{\mathrm{OF}}\alpha_{\mathrm{OF}}\chi}+\cdot\Gamma_{\mathrm{OF}}\log_2\left(\frac{\lambda_2}{L_1}\right)+\Gamma_{\mathrm{OF}}\frac{\alpha_{\mathrm{OF}}M_{\mathrm{OF}}}{\lambda_2}\chi=0.\tag{33}$$

After some mathematical simplifications, the 2^{nd} -order equation is rewritten as:

$$u_1\chi^2+u_2\chi+u_3=0\tag{34}$$

Where:

$$\cdot u_1 := \Gamma_{\mathrm{OF}}\alpha_{\mathrm{OF}}M_{\mathrm{OF}}\left(\frac{\alpha_{\mathrm{OF}}M_{\mathrm{OF}}}{\lambda_2}-\frac{1}{\ln(2)}\right),$$

$$\cdot u_2 := \Gamma_{\mathrm{OF}}\alpha_{\mathrm{OF}}M_{\mathrm{OF}}\left(2.443+\log_2\left(\frac{\lambda_2}{L_1}\right)+\frac{\lambda_4C_{\mathrm{FSO}}}{\Gamma_{\mathrm{OF}}M_{\mathrm{OF}}}\right),$$

$$\cdot u_3 := \Gamma_{\mathrm{OF}}\alpha_{\mathrm{OF}}M_{\mathrm{OF}}\left(\frac{\lambda_2}{\alpha_{\mathrm{OF}}M_{\mathrm{OF}}}\log_2\left(\frac{\lambda_2}{L_1}\right)\right).$$

By using the 2^{nd} order equation's solution (i.e., $\chi=-u_2-\frac{\sqrt{u_2^2-4u_1u_3}}{2u_1}$), and plugging the defined parameters given in Eq. (34) into the solution, Eq. (19) is obtained.

Appendix C.

Similar to Appendix B, the objective function is:

$$\Lambda\left(N,M_{\mathrm{OF}}\right)=\frac{\log_2\left(1+\dfrac{L_1}{\kappa_1-\kappa_2M_{\mathrm{OF}}}\right)}{\kappa_3+\kappa_4M_{\mathrm{OF}}},\tag{35}$$

where the parameters are defined in Eq. ().

To find the optimal value of M_{OF} for a given N, we drive the following first derivative:

$$\begin{aligned}\frac{d}{dM_{\mathrm{OF}}}\left\{\Lambda\left(N,M_{\mathrm{OF}}\right)\right\}&=\frac{d}{dM_{\mathrm{OF}}}\left\{\frac{\log_2\left(1+\dfrac{L_1}{\kappa_1-\kappa_2M_{\mathrm{OF}}}\right)}{\kappa_3+\kappa_4M_{\mathrm{OF}}}\right\}\\&=\left(\kappa_3+\kappa_4M_{\mathrm{OF}}\right)\frac{\kappa_2L_1}{\left(\kappa_1-\kappa_2M_{\mathrm{OF}}\right)\left(\kappa_1-\kappa_2M_{\mathrm{OF}}+L_1\right)\ln(2)}\\&+\kappa_4\log_2\left(1-\frac{L_1}{\kappa_1-\kappa_2M_{\mathrm{OF}}+L_1}\right)\\&\overset{(a)}{\approx}\left(\kappa_3+\kappa_4M_{\mathrm{OF}}\right)\frac{\kappa_2L_1}{\left(\kappa_1-\kappa_2M_{\mathrm{OF}}\right)\left(\kappa_1-\kappa_2M_{\mathrm{OF}}+L_1\right)}\\&-\kappa_4\frac{L_1}{\kappa_1-\kappa_2M_{\mathrm{OF}}+L_1}\\&=\frac{L_1}{\kappa_1-\kappa_2M_{\mathrm{OF}}+L_1}\left(\frac{\kappa_2\left(\kappa_3+\kappa_4M_{\mathrm{OF}}\right)}{\left(\kappa_1-\kappa_2M_{\mathrm{OF}}\right)}-\kappa_4\right)\\&=0,\end{aligned}\tag{36}$$

where (a) holds by using $\ln(1+x)\approx x$ for $x\ll 1$. By solving Eq. (36), we obtain the solution given in Eq. (20). Note that the derived optimal solution is correct for $\kappa_1\kappa_4\geq\kappa_2\kappa_3$. For large values of N, we have $\kappa_1\kappa_4<\kappa_2\kappa_3$ which results $M_{\mathrm{OF}}^{*}=0$.

REFERENCES:

[1] Marzetta, T.L., *Noncooperative Cellular Wireless with Unlimited Numbers of Base Station Antennas.* IEEE Transactions on Wireless Communications, 2010. **9**(11): p. 3590-3600.

[2] Khormuji, M.N., *Generalized Semi-Orthogonal Multiple-Access for Massive MIMO.* IEEE 81st Vehicular Technology Conference, 2015.

[3] Marzetta, H.Q.N.A.A.H.Y.E.G.L.T.L., *Cell-Free Massive MIMO Versus Small Cells.* IEEE Transactions on Wireless Communications, 2017. **16**(3): p. 1834-1850.

[4] Khormuji, A.K.M.J.E.M.N., *Optimal Design of Semi-Orthogonal Multiple-Access Massive MIMO Systems.* IEEE Communications Letters, 2017. **21**(10): p. 2230-2233.

[5] Duong, T.C.M.H.Q.N.M.E.T.Q., *Pilot Power Control for Cell-Free Massive MIMO.* IEEE Transactions on Vehicular Technology, 2018. **67**(11): p. 11264-11268.

[6] D'Andrea, S.B.C., *Cell-Free Massive MIMO: User-Centric Approach.* IEEE Wireless Communications Letters, 2017. **6**(6): p. 706-709.

[7] D'Andrea, S.B.C., *User-Centric Communications versus Cell-free Massive MIMO for 5G Cellular Networks.* 21th International ITG Workshop on Smart Antennas, 2017.

[8] D'Elia, S.B.C.D.A.A.Z.C., *User-Centric 5G Cellular Networks: Resource Allocation and Comparison With the Cell-Free Massive MIMO Approach.* IEEE Transactions on Wireless Communications, 2019. **19**(2).

[9] Larsson, H.Q.N.L.-N.T.T.Q.D.M.M.E.G., *On the Total Energy Efficiency of Cell-Free Massive MIMO.* IEEE Transactions on Green Communications and Networking, 2017. **2**(1): p. 25-39.

[10] Marzetta, H.Y.T.L., *Energy Efficiency of Massive MIMO: Cell-Free vs. Cellular.* IEEE 87th Vehicular Technology Conference, 2018.

[11] Emadi, H.M.M.J., *Performance Analysis of Cell-Free Massive MIMO System With Limited Fronthaul Capacity and Hardware Impairments.* IEEE Transactions on Wireless Communications, 2019. **19**(2): p. 1038-1053.

[12] Xiao, M.B.K.C.A.G.B.H.Q.N.M.D.P., *Max–Min Rate of Cell-Free Massive MIMO Uplink With Optimal Uniform Quantization.* IEEE Transactions on Communications, 2019. **67**(10): p. 6795-6815.

[13] Leung, M.Z.H.M.J.H.J.C.V.C.M., *Statistical Delay-QoS Aware Joint Power Allocation and Relaying Link Selection for Free Space Optics Based Fronthaul Networks.* IEEE Transactions on Communications, 2017. **66**(3): p. 1124-1138.

[14] Uysal, M.A.K.M., *Survey on Free Space Optical Communication: A Communication Theory Perspective.* IEEE Communications Surveys & Tutorials, 2014. **16**(4): p. 2231-2258.

[15] Alouini, A.D.H.D.T.Y.A.-N.M.-S., *Hybrid Radio/Free-Space Optical Design for Next Generation Backhaul Systems.* IEEE Transactions on Communications, 2016. **64**(6): p. 2563-2577.

[16] Alouini, M.U.H.-C.Y.M.-S., *Practical Switching-Based Hybrid FSO/RF Transmission and Its Performance Analysis.* IEEE Photonics Journal 2014. **6**(5).

[17] Schober, V.J.D.S.M.M.U.R., *Link Allocation for Multiuser Systems With Hybrid RF/FSO Backhaul: Delay-Limited and Delay-Tolerant Designs.* IEEE Transactions on Wireless Communications, 2016. **15**(5): p. 3281-3295.

[18] Hranilovic, K.A.S., *C-RAN uplink optimization using mixed radio and FSO fronthaul.* IEEE/OSA Journal of Optical Communications and Networking, 2018. **10**(6): p. 603-612.

[19] Schober, M.N.V.J.R., *Optimal Relay Selection for the Parallel Hybrid RF/FSO Relay Channel: Non-Buffer-Aided and Buffer-Aided Designs.* IEEE Transactions on Communications, 2017. **65**(7): p. 2794-2810.

[20] Uysal, R.C.K.O.N.M., *Centralized Light Access Network (C-LiAN): A Novel Paradigm for Next Generation Indoor VLC Networks.* IEEE Access, 2017. **5**: p. 19703-19710.

[21] Pollin, J.B.A.G.Q.W.D.J.D.G.S., *DenseVLC: a cell-free massive MIMO system with distributed LEDs.* 14th International Conference on emerging Networking EXperiments and Technologies, 2018: p. 320-332.

[22] Pouya Agheli, M.J.E., Hamzeh Beyranvand, *Performance Analysis of Cell-free and User-Centric MIMO Networks with Optical Fronthaul and Backhaul Links.* arXiv preprint arXiv:2011.06680, 2020.

[23] Dhillon, C.S.M.A.H.S., *Bandwidth Partitioning and Downlink Analysis in Millimeter Wave Integrated Access and Backhaul for 5G.* IEEE Transactions on Wireless Communications 2018. **17**(12): p. 8195-9210.

[24] Zorzi, M.P.M.G.A.R.D.C.M., *Distributed Path Selection Strategies for Integrated Access and Backhaul at mmWaves.* IEEE Global Communications Conference, 2018.

[25] Zorzi, M.P.M.G.T.Z.A.R.S.G.D.C.M., *Integrated Access and Backhaul in 5G mmWave Networks: Potential and Challenges.* IEEE Communications Magazine 2020. **58**(3): p. 62-68.

[26] Renaud, L.G.G.M.M.T.L.M.J.F.A.J.S.R.L.I.H.W.R .V.P.C.C., *Integrated Wireless-Optical Backhaul and Fronthaul Provision Through Multicore Fiber.* IEEE Access, 2020. **8**: p. 146915-146922.

[27] Dhillon, C.S.H.S., *Millimeter Wave Integrated Access and Backhaul in 5G: Performance Analysis and Design Insights.* IEEE Journal on Selected Areas in Communications, 2019. **37**(12): p. 2669-2684.

[28] Cover, J.A.T.T.M., *Elements of information theory.* John Wiley & Sons,, 2012.

[29] T. L. Marzetta, E.G.L., H. Yang, and H. Q. Ngo, *Fundamentals of massive MIMO*. 2016: Cambridge: Cambridge University Press.

HOW TO CITE THIS ARTICLE

P. Agheli, M. Emadi, H.Beyranvand, Designing Cost- and Energy-Efficient Cell-free Massive MIMO Network with Fiber and FSO Fronthaul Links, AUT J. Elec. Eng., 53(2) (2021) 159-170.

DOI: 10.22060/eej.2021.19273.5388